

Motivation

Genetically modified T cells expressing chimeric antigen receptors (CARs) specific for tumor associated antigens (TAA) have shown to be effective in treatment of various B cell malignancies, however their safety and clinical efficacy against solid tumors still remains poor. The performed experiments helped us understand in what ways currently evolving chimeric antigen receptor T cell based therapies may be superior to the clinically approved state of the art antibody treatments and how they function at the molecular level. Our results summarized below are important in designing future CAR trials where the optimized constituents of the CAR construct and mode of CAR T cell generation allows striking the required balance between efficacy, endurance and persistence. We have also reviewed the development, current status and perspectives of the field for a special issue of *Biologia Futura* (1).

Establishing and optimizing model systems

First we have successfully designed and retrovirally expressed HER2 specific chimeric antigen receptors without (first generation) or with CD28 or/and 41BB (second and third generation) costimulatory endodomains and have validated the target specific activation and killing ability of the transduced T cells from healthy human donors. Based on the original proposal, we initially tested various HER2-specific CAR molecules that consist of CH2CH3 long hinges. Although these constructs were really easy to label with immunofluorescence for

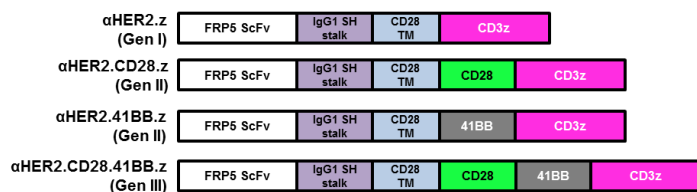


Fig 1. The 3 generations of α HER2 CARs

microscopic evaluation, their target dependent activation based on IL-2 and INF γ release measurements was not sufficient. Thus we decided to move to HER2-specific CARs with an IgG1 short hinge that are

more difficult to label, but proved to be efficient in T cell activation (**Fig. 1**). We have optimized expansion conditions and found that a mixture of recombinant human interleukin IL-7 and IL-15 provides better long term survival than the usual IL-2 based protocol. The initially applied co-culture based transfection was stepped up to a RetroNectin based protocol which both improved efficiency and afforded the absence of contaminating HEK cells. The optimized transduction protocol yielded cells with over 90% CD3 positivity and 60-90% HER2-CAR positivity as well similar expression levels for all CAR generations in both CD4+ and CD8+ T cells.

To be able to quantitate cytotoxic activity against adherent cells on the target cell's side, we have systematically compared the currently available non-radioactive analysis methods. Our results indicated that impedance-based detection is superior to release, membrane permeability, or caspase activation assays (2). In order to investigate in vivo the cytolytic activity of HER2 specific CAR T cells we generated HER2 positive target (MDA-HER2, N87 and JIMT1) and HER2 negative control (MDA) tumor cell lines that stably express the firefly luciferase enzyme (ffLuc) or TurboFP635 (Katushka far red fluorescent protein). Following multiple rounds of cell sorting the reporter protein expression was higher than 95% in all

modified cell lines. We have also established a luminescence-based cytotoxicity assay based on these fLuc modified target cell lines, which makes it possible to determine in vitro CAR T cell cytotoxicity on adherent cultures. Although not informative about the kinetics of killing as the impedance-based assay, this approach gives precise end point results, and is cheaper and easier to perform at higher throughput.

Preclinical efficacy in antibody therapy-resistant models

Since clinical use of CAR T therapy carries the danger of various serious adverse events (SAE), it is highly important to clarify its indications. The more conventional treatment with HER2 targeted monoclonal antibodies often improves the outcome for advanced breast cancer patients, only cases resistant to this therapy may need treatment with HER2-specific CAR T cells. As epitope masking and steric hindrance to antibody binding through ECM components are thought to be the major mechanism of resistance, we asked whether tumors resistant to trastuzumab can still be eliminated by CAR T cells redirected by the same antibody domain. Human T cells were engineered with a CD28-zeta CAR that targets HER2 by a trastuzumab-derived scFv. The reason do diverge from the already optimized FRP5 scFv was to equip the CAR with the

binding avidity exactly the same as the therapeutic antibody to which its efficacy needed to be compared. While saturating doses of trastuzumab in the presence of NK-92 effector cells and also trastuzumab derived CAR T cells equally well recognized and killed HER2-positive tumor cells in vitro in a monolayer, only CAR T cells penetrated in vitro into the core region of tumor spheroids and exhibited cytotoxic activity, whereas antibodies failed. In NSG mice, treatment

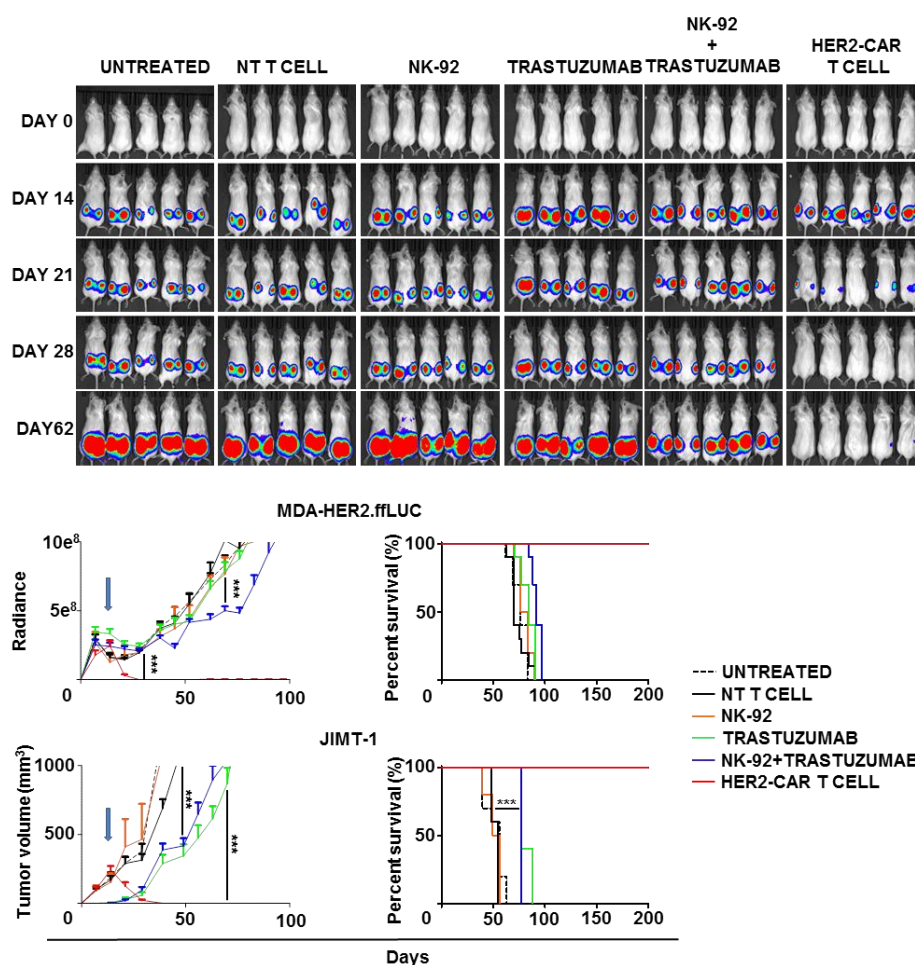


Fig 2. Preclinical efficacy of HER2 targeted CAR T cells in trastuzumab-resistant models

with trastuzumab and NK-92 cells only transiently retarded growth but did not induce regression of clinically trastuzumab-resistant breast cancer xenografts. In contrast, one dose of HER2-specific CAR T cells eradicated established tumors resulting in long-term survival (**Fig. 2**). These data indicated that CAR T cells can successfully combat antibody resistant tumors by targeting the same epitope, suggesting that CAR T cells can efficiently penetrate the tumor matrix that is a barrier for antibodies, and are thus a viable option for the treatment of therapy refractory tumors (3). We have also shown that a small number of HER2 redirected CAR T cells vastly improves the immune response of adoptively transferred syngeneic mouse lymphocytes against the JIMT-1 human breast cancer xenografts (4). This is an important consideration in the construction of TRUCKs (T cells redirected for universal cytokine-mediated killing) and can help localize the cytokine release syndrome (CRS) which is necessary for tumor killing but may have severe systemic side effects.

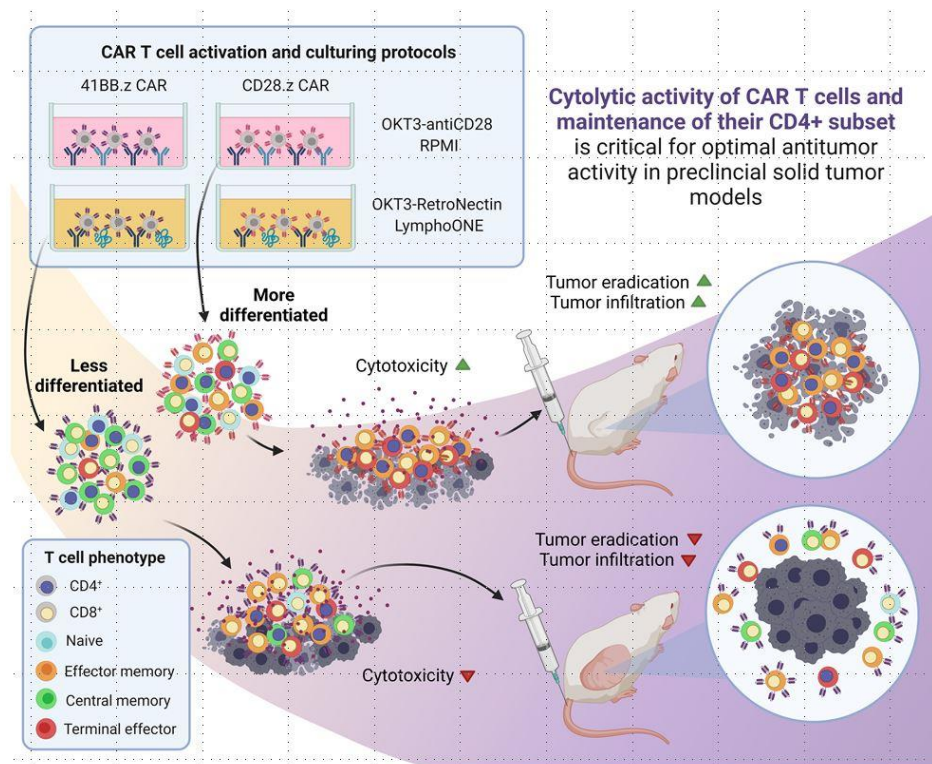
Establishing in vitro and in vivo NK-92 based models for investigating the major in vivo mechanism of action of humanized therapeutic antibodies against HER2 positive tumors has provided opportunity for a joint project establishing a repurposing screen of 774 clinically used compounds on NK-cell + trastuzumab-induced killing of JIMT-1 breast cancer cells. We have found that the multitargeted tyrosine kinase inhibitor sunitinib inhibits ADCC in this model both by suppressing NK cell activation as validated in our cell-free HER2-targeting assay, and by downregulation of HER2 on the target cells' surface and triggering the autophagy pathway. Thus, our data urge caution concerning potential combinations of ADCC-based immunotherapies and sunitinib (5).

Differentiation as an important factor in tumor eradication by CAR T cells

Regarding long term protection by CAR T cells, formation of memory subtypes is expected to be an important factor. Therefore, we have investigated whether the differentiation state (naïve, central memory or effector memory) has any impact on the in vitro and in vivo effector functions. Using different stimulatory protocols (anti-CD3/anti-CD28 or anti-CD3/Retronectin) in combination with various cell culture environment (RPMI or LymphoOne Xeno-Free medium) we have generated CD28z and 41BBz CAR T cell products expressing different memory phenotypes as assessed based on their surface markers. Pre-activation with anti-CD3 and Retronectin in the presence of LymphoOne Xeno-free medium resulted in a CAR T cell product rich in central memory T cells. Canonical anti-CD3/anti-CD28 stimulation combined with RPMI induced higher baseline activation and a well differentiated CAR T cell product with higher percentage of effector memory phenotypes.

Next, we compared the effector functions and killing potential in coculture assays and the long term persistence in rechallenge assay. We found that in CD28z and 41BBz CAR T cell products that are dominated by central memory T cells, lower amount of interferon gamma and interleukin-2 cytokines were released in the presence of the HER2 target antigen. Confirming this result, CAR T cell populations rich in central memory cells induced less efficient killing, but proliferated longer in rechallenge assays. Finally, we have translated these in vitro findings to a HER2 positive breast cancer xenograft model. We monitored the growth of HER2 positive, firefly (ffLUC) modified JIMT1 tumor cells and in a separate

experiment the proliferation of firefly luciferase (ffLUC) expressing CAR T cells. We found that treatment with CD28z or 41BBz CAR T cell products rich in effector memory T cells induced earlier proliferation of effector cells and sequentially eliminated HER2 positive tumor xenografts faster



than products dominated by central memory T cells. Of note, these T cell products contained a significantly higher proportion of CD4+ cells (6), collectively suggesting that higher cytolytic activity and a more pronounced helper subset may be the key to overcoming the potentially immune suppressive tumor microenvironment of solid tumors (Fig. 3).

While from the clinical point of view immediate therapeutic benefits would have priority over efficient response to recurrent tumors, it remains to be seen how the balance between efficacy and long term memory can be stroke by combining various costimulatory domains.

Optimal combination of costimulatory domains

In order to reveal which CAR endodomain composition induces the best T cell activation *in vitro*, we recorded the release of interferon gamma (IFN γ) and interleukin-2 (IL-2) cytokines and cytotoxicity towards target cells as key effector functions. CD28.z CARs induced the highest amount of cytokine secretion and 41BB.z CARs were superior to CARs without costimulatory endodomains. The presence of costimulatory endodomains did not improve short term CAR specific cytotoxicity *in vitro* against monolayer target cell cultures, in contrast to improved cytokine production in this coculture. Next, we performed a rechallenge assay to investigate the role of CD28 and 41BB costimulatory endodomains on HER2-CAR T cell proliferation and exhaustion *in vitro*. HER2-CAR T cells were twice weekly restimulated on immobilized HER2-Fc molecules or with fresh JIMT-1 or N87 targets in 1:1 E:T ratio without cytokine supplementation. NT T cells and MDA cells served as controls. Confirming the ELISA findings, α HER2.CD28.z and α HER2.41BB.z CARs surpassed α HER2.z CARs as judged by fold expansion and cytotoxicity CD28.z CARs induced the best expansion regardless of the target. In parallel, 41BB.z CAR T cells persisted 10 days longer on

immobilized HER2-Fc, however, this effect was not pronounced in cocultures with tumor cells. In parallel, we characterized the effector and memory phenotype pattern of the CAR T cell products on days 0, 3.5, 10.5 and 17.5 of the rechallenge in coculture and found no

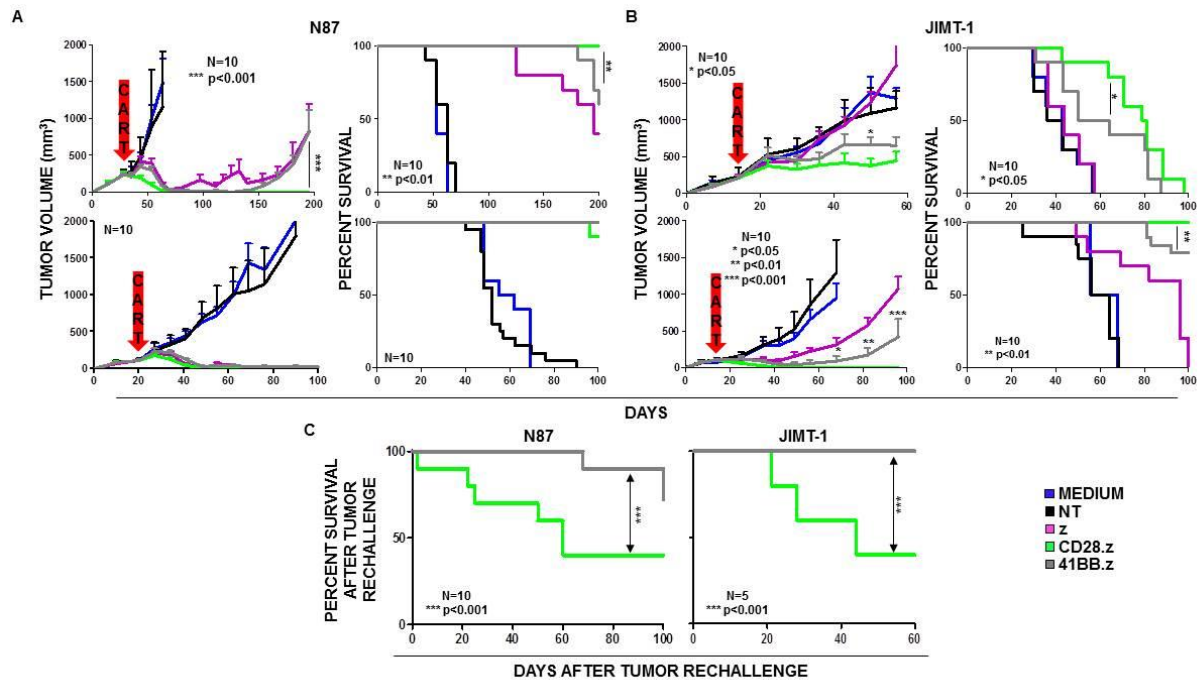


Figure 4. CD28.z CARs induced superior anti-tumor activity, while 41BB.z CAR T cells developed CAR T cell memory in vivo significant differences.

Since CD28.z and 41BB.z CAR T cells exhibited similar anti-tumor activity in vitro, we next investigated whether the expression of various costimulatory endodomains results in different efficacies in tumor elimination in vivo. First, we established subcutaneous HER2⁺ N87 and JIMT-1 xenograft models in NSG mice. To test the cytolytic function, a single dose of 2×10^6 HER2-CAR T cells were applied i.v. on the day when tumor volume reached 250mm³ (large tumor model, **Fig. 4A,B** upper panels) or 125mm³ (small tumor model, **Fig. 4A,B** bottom panels). We observed that CD28.z CAR T cells induced better anti-tumor activity and improved overall survival in large N87, large JIMT-1 and small JIMT-1 tumor models than any other HER2-CAR treatment ($p < 0.05$). We rechallenged the animals that were tumor free on day 100 with 2×10^6 JIMT-1 or N87 tumor cells without CAR reinjection to investigate the development of *in vivo* CAR T cell memory. We observed that in both tumor groups 41BB.z CAR T cells prevented the animals from tumor recurrence ($p < 0.001$, grey lines, **Fig. 4C**).

Next, we modified our small tumor model to investigate simultaneously the growth of HER2⁺ xenografts and the persistence of CD28.z and 41BB.z CAR T cells. For this, we have generated JIMT-1 and N87 cell lines that stably expressed Katushka2S far-red fluorescent proteins (JIMT-1.katushka and N87.katushka) {Kalinina, 2018 #169}. In parallel NT and CAR T cells were genetically modified to express the ffLuc reporter (HER2-CAR.ffLuc).

Thus, we could detect tumor specific far-red fluorescence and T cell derived luminescence at the same time (**Fig. 5A**). We observed that CD28.z CARs induced faster CAR T cell expansion in both xenograft models (green lines HER2-CAR.ffLuc, **Fig. 5B,C**) and this robust expansion persisted for three weeks in mice bearing JIMT-1 tumors (green lines HER2-CAR.ffLuc, **Fig. 5C**).

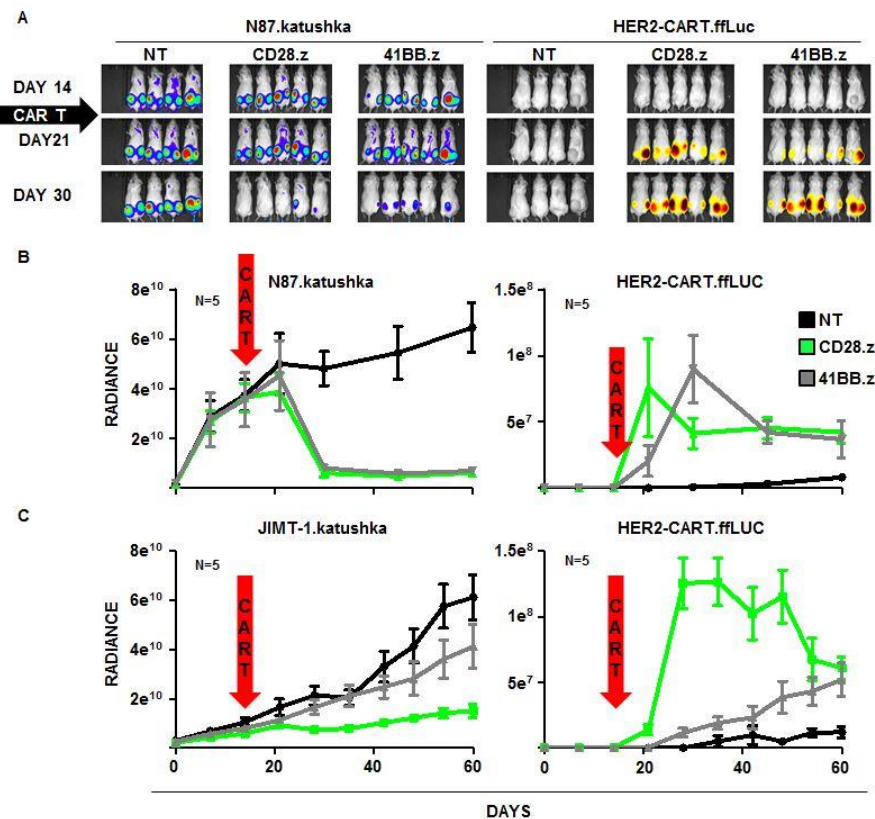


Figure 5. Simultaneous in vivo detection of CAR T cell expansion and tumor regression

In order to benefit from both the CD28 driven robust tumor cell elimination and the 41BB derived long-term anti-tumor effects we combined the two costimulatory endodomains in one CD28.41BB.z CAR construct and also co-administered them as a 1:1 ratio mixture of CD28.z and 41BB.z CAR T cells. (**Fig. 6A**). The third generation α HER2.CD28.41BB.z CAR containing both costimulatory endodomains (**Fig. 6B**) exhibited a 65.6% mean transduction efficiency that was similar to the other HER2-CARs (**Fig. 6C**), however its expression level was the lowest among the constructs. We did not detect a higher percentage of CD8⁺ cytotoxic cells or larger initial proportions of the effector memory phenotype in CD28.41BB.z and mixed (CD28.z + 41BB.z) CAR T cell populations. Next, we compared the *in vitro* effector functions of the α HER2.CD28.41BB.z CAR T cells with the mixed α HER2.CD28.z and α HER2. 41BB.z CAR T cell product. We incubated the effector cells on 1 μ g/ml immobilized HER2-Fc chimera protein coated plates or with HER2⁺ target cells in 1:1 effector to target (E:T) ratio for 24 hours to determine IFN γ and IL-2 secretion. HER2⁻ MDA cells served as controls. We found that both CAR products induced a CD28.z like robust IFN γ and IL-2 production in the presence of target (**Fig. 6D,E**). Moreover, in cocultures with HER2⁺ tumor cells the 1:1 mixture of CD28.z and 41BB.z CAR T cells secreted the highest amount of IL-2 (**Fig. 6E**). However, we could not differentiate between any of the CAR T cell products based on their short term cytolytic activity *in vitro*. In rechallenge assay the immobilized HER2-Fc antigen induced better expansion of mixed CD28.z and 41BB.z CAR T cells than CD28.41BB.z CARs (**Fig. 6F**). CD28.41BB.z CAR T cells or the mixture of CD28.z and 41BB.z CAR T cells were not activated in the presence of HER2⁻ MDA target cells, but have

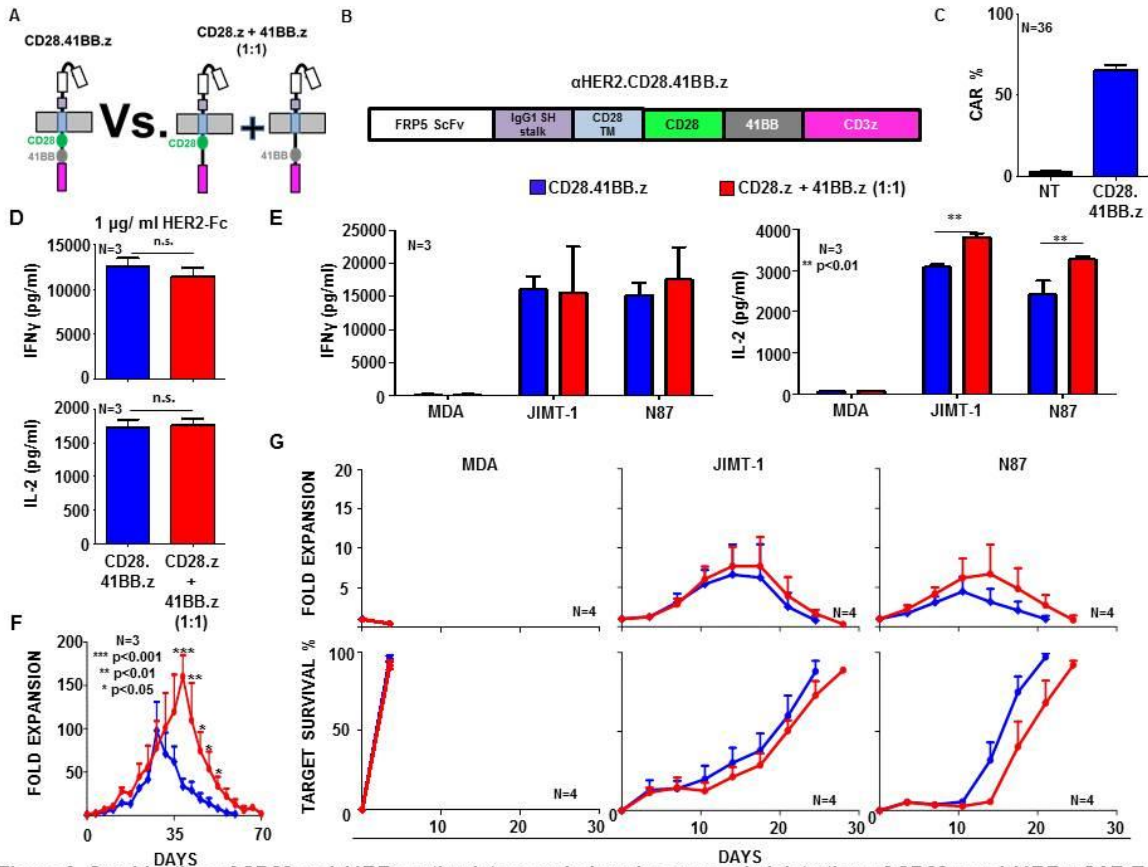


Figure 6. Combination of CD28 and 41BB costimulatory endodomains or co-administration of CD28.z and 41BB.z CAR T cells induce robust T cell activation in vitro

shown robust and comparable cytotoxicity following sequential stimulation with HER2⁺ tumor cells (**Fig. 6G**). We concluded that of all first, second and third generation CAR constructs, the 1:1 ratio mixture of CD28.z + 41BB.z CAR T cells induced the longest persistence with the most potent cytotoxicity (**red lines, Fig. 6D**).

Next, we investigated whether the combination of CD28 and 41BB costimulatory endodomains could also improve in vivo anti-tumor functions. Thus, we induced subcutaneous N87.ffLuc and JIMT-1.ffLuc small tumor xenografts in NSG mice (**Fig. 7A**). We found that both CD28.41BB.z and a 1:1 mixture of CD28.z + 41BB.z CAR T cells induced robust anti-tumor activity resulting in complete and long term tumor eradication (**Fig. 7B,C**). However, on week 12 one animal in the CD28.41BB.z group that developed >15% weight loss, hunched posture, fur loss, reduced mobility, and other clinical symptoms of GvHD was sacrificed, (blue trace in Kaplan-Meyer plot, **Fig. 7C**). Following rechallenge of the tumor free animals on day 100 after the first tumor inoculation, the mixed population of CD28.z and 41BB.z CAR T cells exhibited better CAR T cell memory against N87 tumor rechallenge ($p < 0.001$, N87.ffLUC, red line, **Fig. 7D**). In the JIMT-1 group, both double costimulated CAR T cell products prevented the animals from tumor recurrence (JIMT-1.ffLUC, red and blue lines lines, **Fig. 7D**). Finally, we monitored simultaneously the tumor development and the persistence of various CAR T cells using Katushka2S labeled tumor cells and ffLuc expressing CAR T cells. We found that the mixture of CD28.z and 41BB.z CAR T cells has shown faster expansion in both xenografts.

To reveal how CD28.z and 41BB.z CAR T cells influence each other's function following tumor recognition, we designed an in vivo experimental approach that allows us to monitor the persistence of CD28.z and 41BB.z CAR T cells alone or in the presence of the other costimulatory CAR T cells. For tracking CD28.z CAR T cells, we generated CAR T cell products consisting of 1 million ffLUC labeled CD28.z CAR T cells with 1 million unlabeled CD28.z or 41BB.z

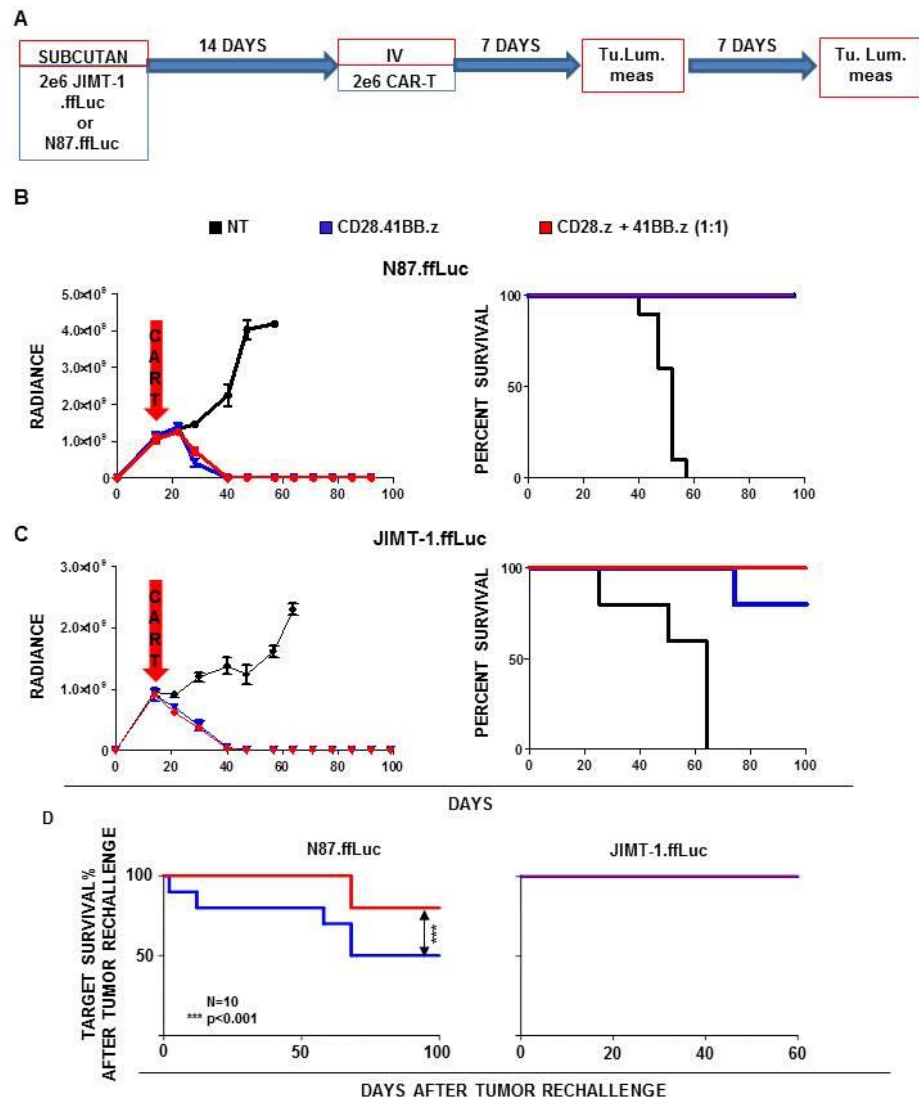


Figure 7. Co-administration of CD28.z and 41BB.z CAR T cells improves in vivo expansion and long term memory over third generation CAR T cells

CAR Ts (left panels, **Fig. 8A,B**). To monitor 41BB.z persistence we mixed 1 million ffLUC labeled 41BB.z CAR T cells with 1 million unlabeled CD28.z or 41BB.z CAR Ts (right panels, **Fig. 8A,B**). CAR T cell products were injected i.v. on day 14 post JIMT-1 xenotransplantation (small tumor model). Interestingly, we found that ffLuc modified CD28.z CAR T cells have shown similar initial expansion in the presence of untagged CD28.z or 41BB.z CAR T cells (left panels, **Fig. 8A,B**). In contrast, ffLuc modified 41BB.z CAR T cells expanded faster in the first two weeks after CAR T cell injection ($p < 0.05$, day 21, day 28, right panels, **Fig. 8A,B**) when they were co-administered with untagged CD28.z CAR T cells and expanded less if the same amount of untagged 41BB.z CAR T cells were present. At this point we would like to highlight that this early post-injection period has key significance in tumor eradication.

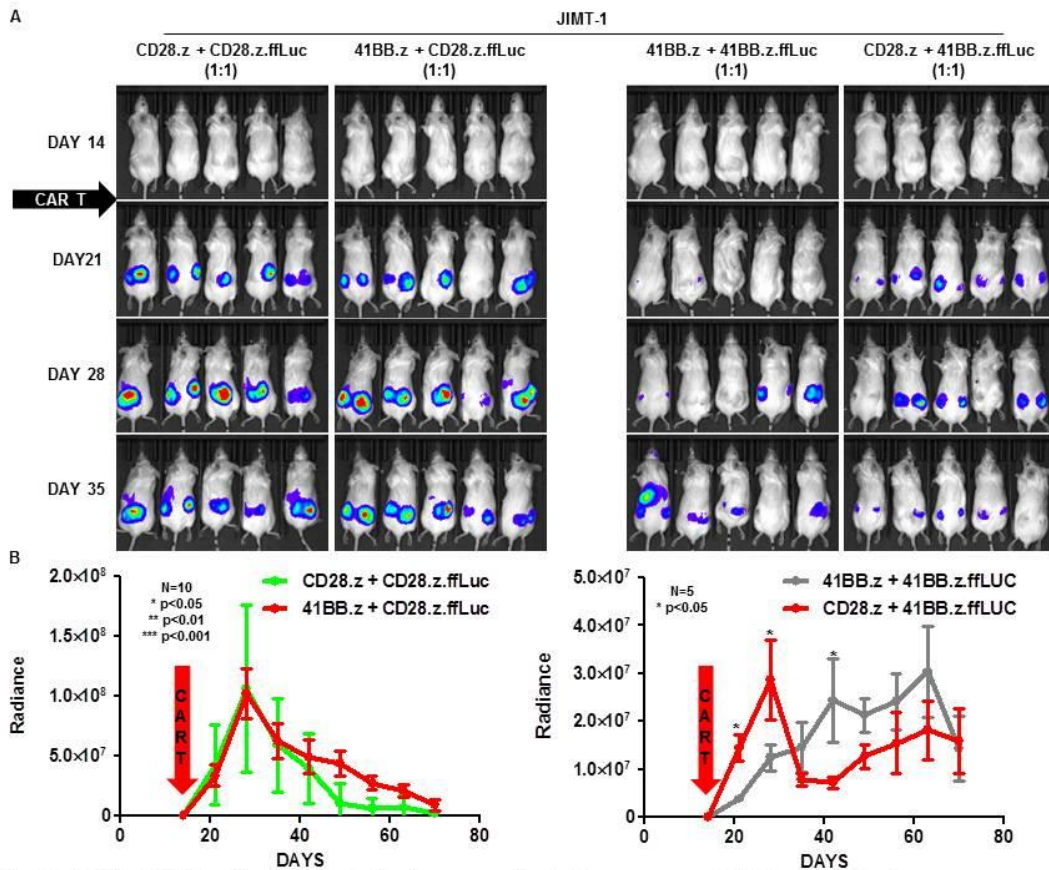


Fig. 8. 41BB.z CAR T cells show faster in vivo expansion in the presence of CD28.z CAR T cells

To reveal potential mechanisms in the background of these observations, we performed multiplex transcriptional profiling of the CD28.z; 41BB.z; CD28.41BB.z and CD28.z + 41BB.z (1:1) CAR T cell products at days 0; 3.5; 7; 14 and 21 of serial activation using the Nanostring nCounter® Immunology Panel (**Fig. 9A**). Using principal component analysis we compared the RNA expression profiles and determined that following 21 days of antigen stimulation the transcriptional pattern of the 41BB.z CAR T cells significantly differed from the other three CAR T cell products (red arrow, **Fig. 9A**). Exploring differences in the T cell specific signaling pathways, we have revealed that interferon and interleukin signaling remained activated in 41BB.z CAR T cells after 21 days of HER2 stimulation (cluster 3, **Fig. 9B** 41BB.z column and **Fig. 9C**) in contrast to the other CAR T cell cultures where these cytokine pathways became quiescent (cluster 3, **Fig. 9B** CD28.z, CD28.41BB.z and CD28.z + 41BB.z columns). Moreover, in the CD28.z population we found an overexpression of the CCL4, LAG3, CTLA4 and ITGA4 exhaustion markers (cluster 2, **Fig. 9B** CD28.z and **Fig. 9C**). Interestingly, the transcriptional profile of CD28.41BB.z CAR T cells is similar to CD28.z with dominant overexpression of BATF and CCL3 exhaustion genes (cluster 1, **Fig. 9B** CD28.z and CD28.41BB.z and **Fig. 8C**). In the CD28.z and 41BB.z mixed population we could not identify such up- or downregulated pathways, the overall gene expression profile was in the midrange of the 41BB.z and CD28.z/CD28.41BB.z profiles (cluster 1, 2 and 3 **Fig. 9B** CD28.z + 41BB.z and **Fig. 9C**).

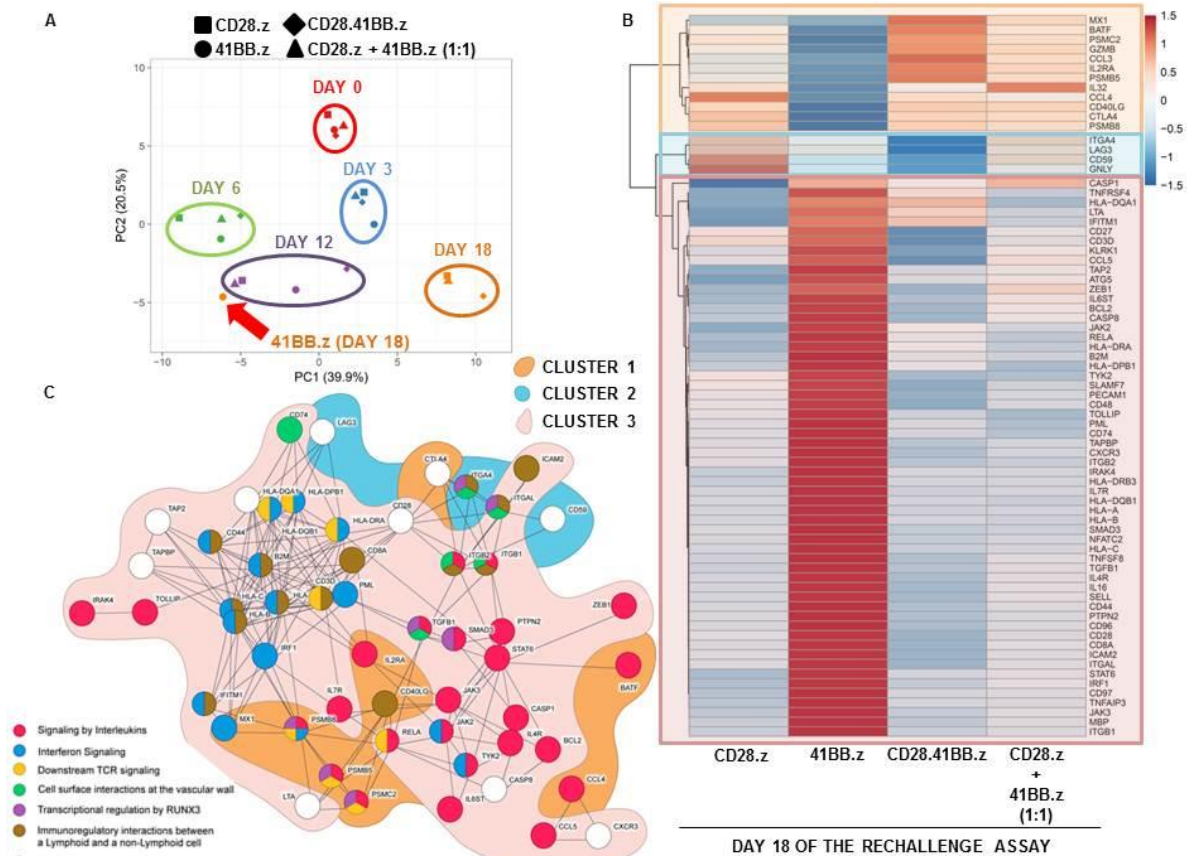


Fig. 9. In a mixed CD28.z + 41BB.z CAR T product cytokine release and T cell exhaustion are under balanced regulation

Overall, we have shown that CD28 costimulation yields more vigorous cytokine release in vitro and more efficient killing of solid tumors in vivo than 41BB costimulation, which, however, confers long term persistence on T cells wielding 41BB.z CARs. These T cells consequently prevent the growth of rechallenge tumor xenografts even two months after the first tumor has been eliminated by them. To improve the success rate of eliminating the primary tumor by 41BB.z CAR T cells, adding the CD28 costimulatory endodomains to yield single efficient 3rd generation CAR is the current state of the art. However, we show that while this strategy improves the initial therapy success in preclinical solid tumors, it does not improve response to tumor rechallenge. Contrary, the co-administration of CD28.z and 41BB.z CAR T cells in 1:1 ratio performs optimally both in eliminating primary tumors and in preventing recurrence. From the mechanistic point of view, in this product the presence of CD28.z CAR T cells enhances also the initial expansion of 41BB.z CAR T cells in the TME, which thereafter can persist in the long run as the primary tumor is efficiently cured. Transcriptional analysis of lymphocyte specific signaling pathways indicates that such mixtures of 2nd generation CAR T cells exhibit a balanced regulation of cytokine secretion and exhaustion which allows for both an efficient initial tumor killing and consecutive long term persistence. These findings inform the design of future clinical trials where understanding the contribution of the various potential constituents of the chimeric receptor construct could be a key to striking the required balance between efficacy, endurance and persistence of the adoptively transferred T cells (7).

Novel molecular targets that may influence the antitumor response

Earlier literature data showed that proliferation and anti-apoptosis of T cells upon target engagement was vastly promoted in subsets where Ppp2r2d, the regulatory subunit of protein phosphatase 2A was spontaneously eliminated. Thus we hypothesized that stably suppressing the expression of this protein could enhance both expansion efficiency and long term persistence of CAR T cells. We used the α HER2-CD28-CD3z and α HER2-41BB-CD3z constructs to transduce the expanded lymphocyte population with an anti HER2 CAR, as well as to co-transduce a vector coding for shRNA against Ppp2r2d. Knockdown efficiency was verified in Western blot. Next we tested CAR T cell functions in short and long term coculture assays. We found that Ppp2r2d-silenced HER2-specific CAR T cells secreted somewhat higher amount of IFN γ in short term coculture assays, however the difference was not significant. In long-term rechallenge assays, these Ppp2r2d silenced CAR T cells did not show improved killing and persistence in comparison to their unsilenced counterparts with either of the 2nd generation CARs. Since there were no functional differences upon knockdown in these assays, this specific aim of our project was completed with negative results. At the same time we've had the opportunity to contribute to a project exploring the role of another novel molecular player, calcium/calmodulin dependent protein kinase 1D (CAMK1D) that can modulate antitumor immunity. It was revealed that expression of CAMK1D in the tumor induces resistance to anti-PD-L1 treatment and conversely, tumors without CAMK1D were eliminated more facily (8). Since CAR T cells are equally exposed to immune checkpoint modulators released by solid tumors as the native T cells, checkpoint blockade may be a viable option for boosting CAR T cell activity. In this context CAMK1D may become an important predictor of therapy outcome, particularly when using checkpoint-edited CRISPR/Cas modified CAR T cells.

Molecular dynamics of the CAR immune synapse

Since not much is known about the dynamics of CAR T cell immune synapses compared to conventional T cell immune synapses, we have investigated the molecular parameters that may influence synapse formation and consequently the efficacy of killing. Initial observations have shown that even though the scFv domains of two different CARs did bind to their respective targets with the same avidity and the CARs were expressed in the cell membrane in similar numbers, CAR redirected activation of T cells was less efficient when targeting HMW-MAA (CSPG4) compared to targeting p97 melanotransferrin (**Fig. 10A**). Fluorescent labeling and confocal microscopy have revealed that HMW-MAA, a large intrinsic chondroitinsulphate-proteoglycan forms large clusters in the cell membrane and strongly colocalizes with GM1 rich lipid rafts as opposed to the GPI-linked p97, which forms small clusters that overlap less with raft microdomains (**Fig. 10B,D**). To characterize the intramembrane mobility of these target molecules, we have developed fluorescence

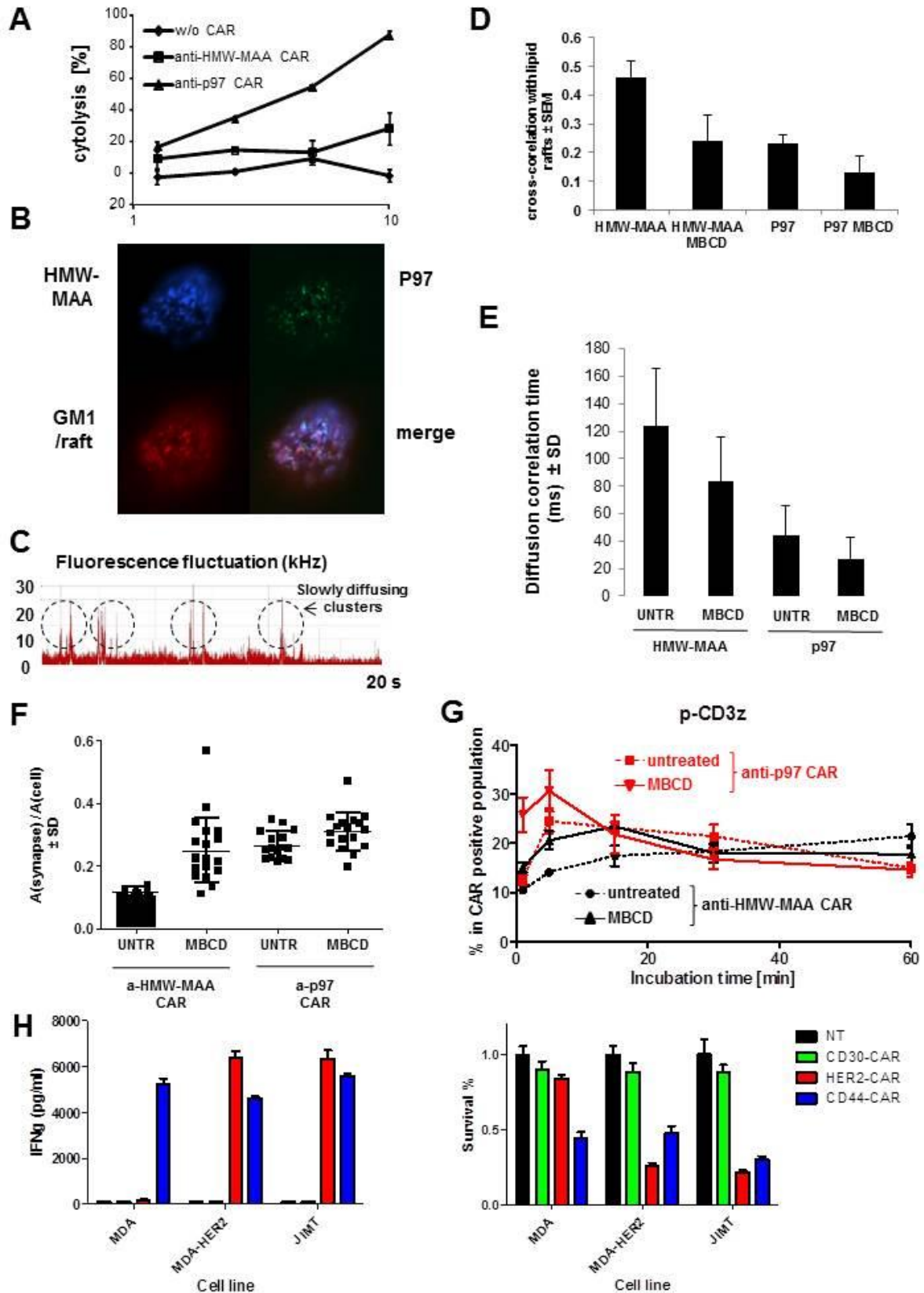


Fig. 10. High mobility and preformed small clusters of target antigens in the membrane enhances synapse formation, CAR T cells activation and cytotoxicity in vitro correlation spectroscopy workflows (9) that allowed the observation of single molecules diffusing in the plane of the membrane as well as larger clusters of molecules that diffused

more slowly and could be identified as higher and broader spikes in the fluctuation of detected signals (**Fig. 10C**). Since P97 showed faster diffusion (short diffusional correlation times, **Fig. 10E**) as well as small preassembled clusters with detectable mobility, whereas HMW-MAA exhibited slower molecular mobility (**Fig. 10E**) and virtually steady lipid-raft-based large clusters, we hypothesized that p97 is more easily collected into the immune synapse giving rise to more efficient CAR-redirection killing through this target. To support this notion, we have treated the target cells with methyl- β -cyclodextrine to extract the cholesterol content of GM1-rich lipid rafts and thereby mobilize the target molecules. This treatment, carefully titrated to preserve cell viability and membrane antigen expression, decreased the overlap of both target molecules with lipid rafts (**Fig. 10D**) and increased their membrane diffusion rate as evidenced by decreased diffusion correlation times (**Fig. 10E**). Mobilizing HMW-MAA in this manner increased the area of CAR T immune synapses relative to target cell area significantly, reaching the values observed for p97 on control cells. Apparently this parameter was already in saturation for p97 as cholesterol extraction did not further increase its synaptic areas (**Fig. 10F**). Since the cells replenish cholesterol in their membrane within an hour, direct readout of cytotoxicity was not possible upon MBCD treatment, so we resorted to measuring immunostained pCD3z, pLCK and pZAP70 as surrogate markers of CAR T cell activation. All these markers have revealed a faster and strong activation upon engagement of p97, and further mobilizing the targets increased this activation both for p97 and HMW-MAA, the latter reaching the level achieved on p97 in untreated cells (**Fig. 10G**). To confirm the established principle that higher mobility of the target increases the rate of formation and stability of immune synapses and through this the efficacy of tumor killing, we have made use of our established in vivo preclinical models.

With the JIMT-1 and MDA-HER2 tumors expressing HER2, the MDA-MB-468 serving as HER2⁻ control, and all of them expressing CD44, we could compare side by side the activation and antitumor efficacy of CAR T cells targeting either HER2 or CD44. CD44 is a heavily glycosylated integral membrane protein which is also hindered in its mobility by binding to hyaluronic acid in the ECM. As opposed to this, HER2 with a single transmembrane alpha helix enjoys free lateral mobility in the membrane, although with a diffusion constant lesser than p97. In vitro data have verified that specific binding of the target by each CAR evokes INF γ release (**Fig. 10H**, left panel), while NT T cells or those with an irrelevant CAR (against CD30) did not induce activation. Furthermore, all relevant CARs evoked tumor cell killing, and the anti HER2 CARs have exhibited stronger cytotoxicity than anti CD44 CARs (**Fig. 10H**, right panel).

These observations entitled us to test our hypothesis in preclinical models as well. We have treated JIMT-1 tumors starting on day 21 post-implantation with a single dose of either HER2 or CD44-redirection CARs, using, for each cohort, either 0.5, or 1 or 2 million CAR T cells. Stably expressed fLuc was used to regularly follow up tumor volume. Non-transduced and CD44-targeted CAR T cells have failed to eliminate tumors, while mice receiving 1 or 2 million HER2-targeted CAR T cells were all cured, and also those receiving 0.5 million CAR T cells showed 80% survival by day 100 (**Fig. 10H**). Interestingly, CD44 CARs have shown even less efficacy compared to HER2 CARs than in vitro. This is likely owed to the 3D

growth of tumors accompanied by the generation of a formidable extracellular matrix, where CD44 binding to hyaluronic acid can further reduce the mobility of this target antigen. These data highlight the importance of prudent target selection during the design of CAR T trials in the treatment of solid tumors. In addition to differential expression of tumor neoantigens (such as, for example, CD44 splice variants), their accessibility and mobility also needs to be taken into account. Specifically, also considering the requirement of a more vigorous tumor elimination (as shown and discussed in previous chapters), targets with high membrane mobility, preformed mobile clusters, and easy recruitment to the immune synapse should be preferred (10).

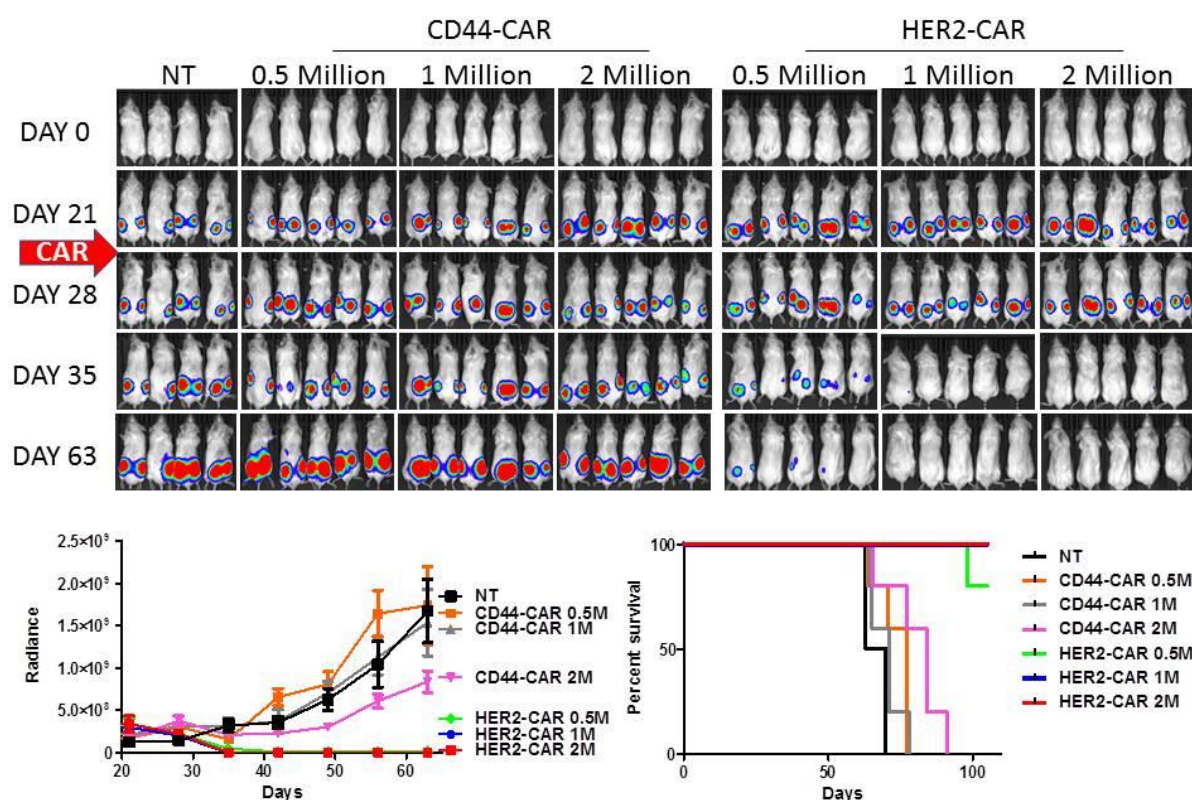


Fig. 11. High membrane mobility of target antigens enhances in vivo antitumor efficacy of CART cells

Since it is reasonable to propose that the dynamics of immune synapse formation and consequential CAR T cell function is also affected by the CAR construct, its mobility and interactions in the cell membrane, we have used our set of 1st, 2nd and 3rd generation anti-HER2 CARs to shed light on potential correlations between molecular level organization and function. First we investigated the membrane distribution of CARs on the surface of unstimulated T cells using semi-superresolution AiryScan microscopy. Approximately 600 nm thin optical slices of the apical membranes were imaged, and then segmented and analyzed (Fig. 12A). The HER2.z CAR without costimulation exhibited slightly higher but not significantly different membrane intensity (Fig. 12B). About 3/4th of the receptors was localized in clusters (Fig. 12C), and of these, the HER2.z clusters showed higher average

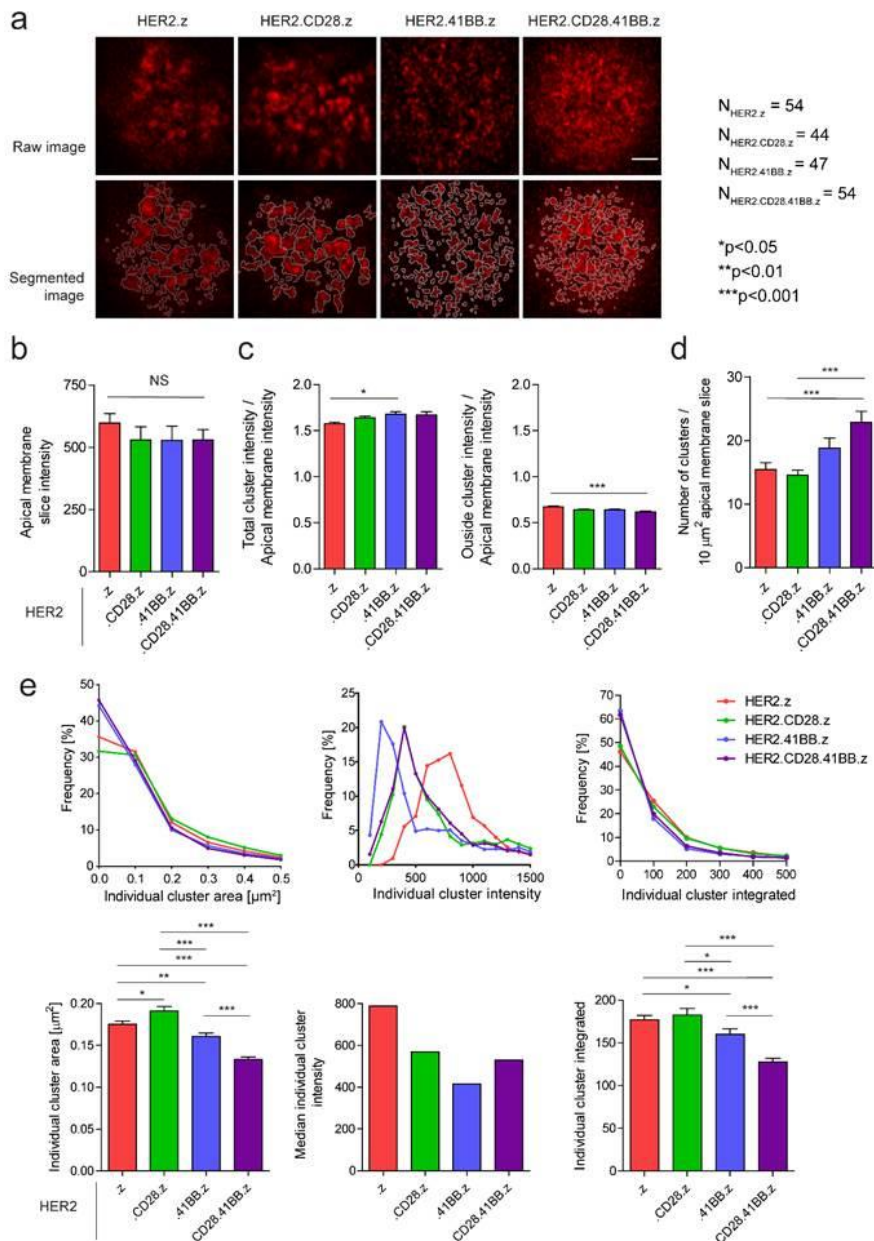


Fig. 12. 41BB containing CAR constructs form more numerous and smaller clusters in the membrane of unstimulated CAR T cells

41BB containing constructs, which had overall smaller spike amplitudes. While this correlates with the observed submicroscopic clusters in AiryScan images, it must be noted that the two methods represent two different levels of aggregation. From the fluctuation traces autocorrelation functions were calculated their ensemble was fitted to a model with two diffusion components and triplet fraction. In this, fraction of the free 3D diffusion of the detached A647 conjugated monomer HER2 used for labeling was fitted, while its diffusional correlation time $\tau_{d,dye}$ was determined in an independent calibration measurement, similarly to the triplet lifetime and fraction. The main parameters of interest for the 2D diffusion of CAR species, its fraction and diffusional correlation time were both determined from the fit (Fig. 13B). Diffusion correlation times were translated to diffusion constants using the calibrated size of the detected confocal volume. The HER2.z construct exhibited significantly slower

intensity possibly reflecting the higher overall expression level (Fig. 12E, middle panels). 41BB containing constructs aggregated in significantly smaller and more numerous clusters (Fig. 12D,E).

Fluorescence correlation spectroscopy was used to analyse the mobility of the receptors in the membrane of living cells. Individual fluctuation traces revealed that HER2.z and HER2.CD28.z constructs frequently formed larger clusters that showed up as larger and longer spikes in the record (Fig. 13A), as opposed to

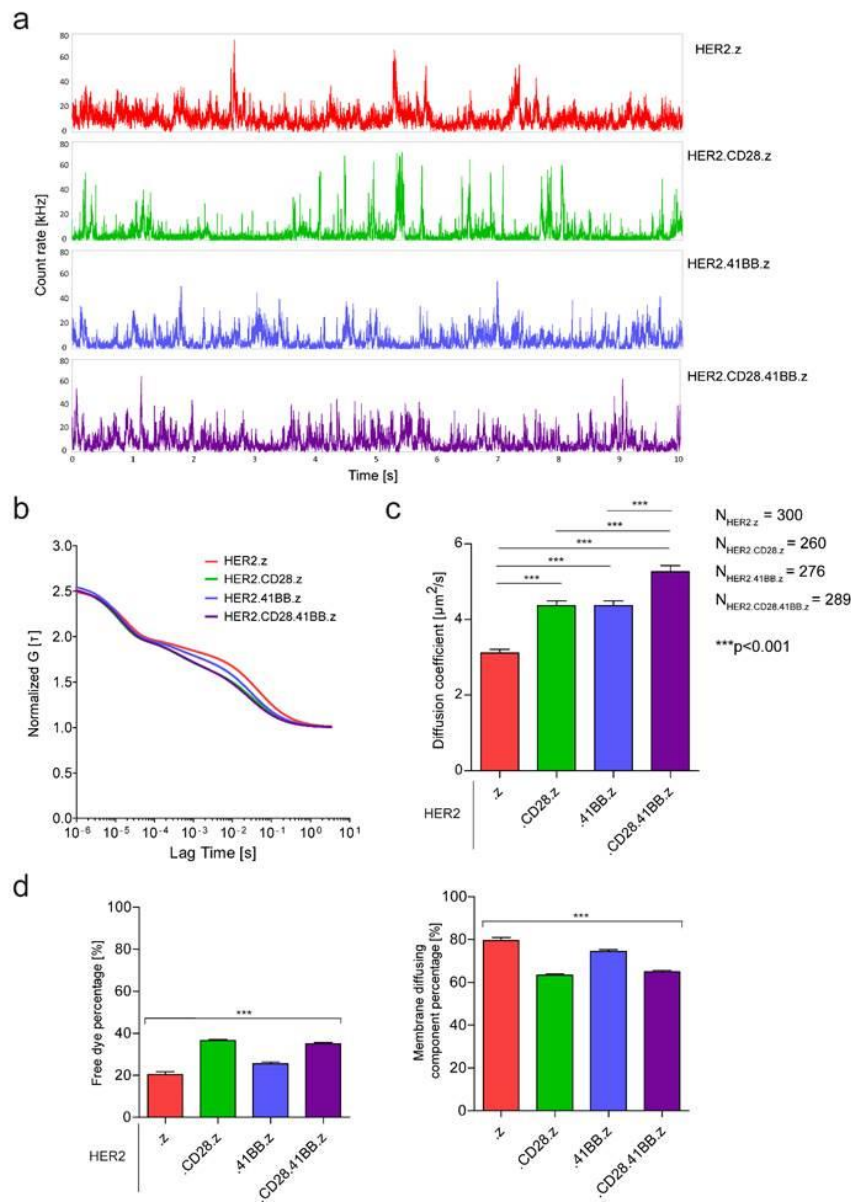


Fig. 13. CD28.41BB gen III CARs are more mobile in the membrane of unstimulated CAR T cells

constructs evoked significantly stronger short term CD3z phosphorylation than the other two constructs, both in terms of average and integrated synaptic intensity (**Fig. 14B**, top row). Integrated intensity of pLck staining followed the same trends, although statistically the differences were not significant (**Fig. 14B**, lower right panel). The pLck signal has spread out to a significantly larger area in the synapse in the case of the HER2.z CAR, which rendered the average synaptic intensity weaker for this construct than for the 3rd generation as HER2.CD28.41BB.z (**Fig. 14B**, bottom row). Overall, this HER2.CD28.41BB.z construct exhibited the most compact, highly activated synapses, which can partly be attributed to the smaller, but more numerous clusters it has already formed before stimulation, as well as having the highest mobility of all the receptors at the sub-cluster/supramolecular level. Looking at the molecular models of the constructs generated by the RoseTTAFold deep learning-based protein structure prediction algorithm (**Fig. 14C**) revealed that the 41BB

diffusion, while the HER2.CD28.41BB.z significantly faster diffusion than the other two constructs (**Fig. 13C**). CD28 bearing constructs consistently showed a larger free fraction of dissociated ligands, possibly indicating that the presence of this domain may reduce the binding affinity of the CAR.

The short term recruitment and activation properties of the constructs was investigated by quantitative fluorescence confocal microscopy, exploiting phospho-CD3z and phospho-Lck specific labeling (**Fig. 14A**). Quantitative image analysis has revealed that the HER2.z and the

HER2.CD28.41BB.z

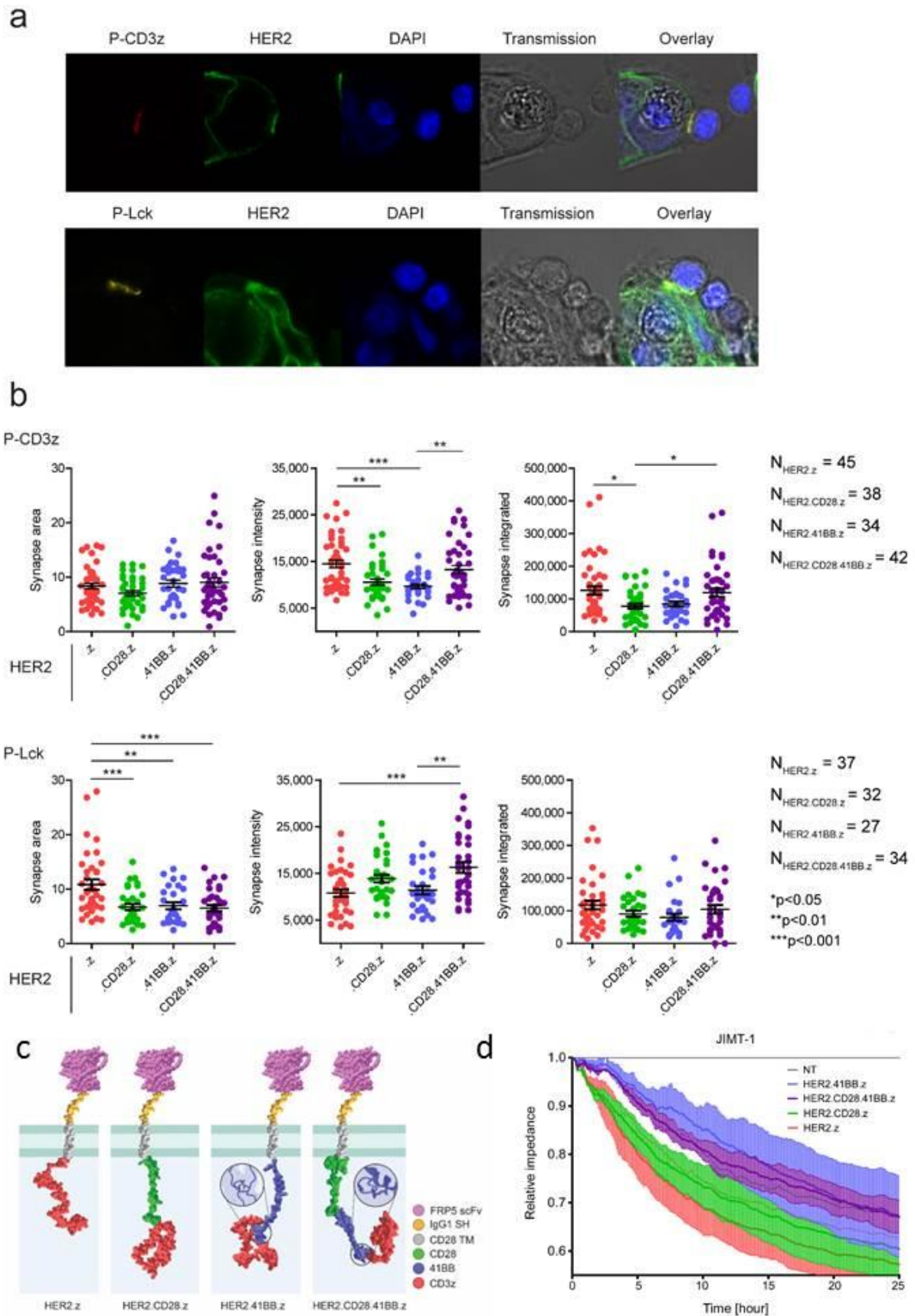


Fig. 14. CD28.41BB gen III CARs show strong short term Lck phosphorylation in compact synapses upon target engagement but do not perform well in long term cytotoxicity

costimulatory domain contains three cysteines, two of which are expected to form an intramolecular disulphide bridge that influences the steric positioning of the CD3z domain, while the third likely mediates the homodimerisation of 41BB containing constructs. In fact, when analyzing the monomer/oligomer ratio in non-reducing vs. reducing Western blot, on average 38% of 41BB.z and 60% of CD28.41BB.z CARs forms oligomers, in contrast to below 10% of CD28.z and .z CARs.

Overall, molecular and functional imaging suggest that 41BB containing CARs homo-oligomerize and these oligomers convene to form smaller but more numerous membrane clusters in resting T cells. Lateral diffusion of the chimeric receptors increases as the CD3z effector domain is removed further and further away from the plane of the membrane, possibly reflecting the diminished interaction of this domain with membrane-associated signaling moieties that belong to, or interact with, the native TCR in these cells. Nevertheless, the slowest moving .z and the fastest moving, but pre-oligomerized CD28.41BB.z CARs are equally capable of inducing fast and stronger than average CD3z phosphorylation, suggesting that higher mobility and pre-assembled building blocks can promote immune synapse formation. Furthermore, these synapses formed by CD28.41BB.z exhibit a more compact region of stronger Lck recruitment and phosphorylation. Interestingly, even though short term activation upon first target cell engagement is most pronounced in T cells redirected by non-costimulated .z and third generation CD28.41BB.z CARs, longer term cytotoxic efficacy is grossly different for these two species (**Fig. 14D**); impedance-based real time monitoring of cell adhesion shows that 1st generation .z CARs confer the most robust target cell killing on T cells (red trace), while CARs wielding 41BB costimulation (blue and purple traces) fare the worst. Cumulatively, these observations underline the importance of mobility, the tendency to form spontaneously oligomers and the ability to engage in membrane-proximal molecular interactions as design parameters predicting efficient synapse formation upon first target engagement. However, there is a caveat that even if these principles are observed, the quality of costimulation becomes the major determinant of CAR T cell efficacy already in the first hours of effector-target co-culture ([11](#)).

Publications with support from NKFIH grant K119690, as cited in the report

1. Szöör, Á., Szöllösi, J., Vereb, G.: From antibodies to living drugs: quo vadis cancer immunotherapy? [Biol. Futura. 72 \(1\), 85-99, 2021.](#) (Q3, IF: 0.821 (2020)) [↗](#)
2. Tóth, G., Szöllösi, J., Vereb, G.: Quantitating ADCC against adherent cells: impedance-based detection is superior to release, membrane permeability, or caspase activation assays in resolving antibody dose response. [Cytom. Part A. 91 \(10\), 1021-1029, 2017.](#) (Q1, IF: 3.26) [↗](#)
3. Szöör, Á., Tóth, G., Zsebik, B., Szabó, V., Eshhar, Z., Abken, H., Vereb, G.: Trastuzumab Derived HER2-specific CARs for the Treatment of Trastuzumab-Resistant Breast Cancer: CAR T Cells Penetrate and Eradicate Tumors That Are Not Accessible to Antibodies. [Cancer Lett. 484 1-8, 2020.](#) (Q1, IF: 8.679) [↗](#)
4. Tóth, G., Szöllösi, J., Abken, H., Vereb, G.*, Szöör, Á.*: A Small Number of HER2 Redirected CAR T Cells Significantly Improves Immune Response of Adoptively Transferred Mouse Lymphocytes against Human Breast Cancer Xenografts. [Int. J. Mol. Sci. 21 \(3\), 1-11, 2020.](#) (D1, IF: 5.923) * equally senior/corresponding authors [↗](#)
5. Guti E., Regdon Z., Sturniolo I., Kiss A., Kovács K., Demény M., Szöör Á., Vereb G., Szöllösi J., Hegedűs C., Polgár Z., Virág L.: The multitargeted receptor tyrosine kinase inhibitor sunitinib induces resistance of HER2 positive breast cancer cells to trastuzumab-mediated ADCC, [Cancer Immunol Immunother](#) doi: 10.1007/s00262-022-03146-z. Online ahead of print, 2022 (Q1, IF: 6.968) [↗](#)
6. Csaplár, M., Szöllösi, J., Gottschalk, S., Vereb, G.*, Szöör, Á.*: Cytolytic Activity of CAR T Cells and Maintenance of Their CD4+ Subset Is Critical for Optimal Antitumor Activity in Preclinical Solid Tumor Models. [Cancers \(Basel\). 13 \(17\), 1-19, 2021.](#) (Q1, IF: 6.639 (2020)) * equally senior/corresponding authors [↗](#)
7. Szöör, Á., Csaplár, M., Gottschalk, S., Vereb, G.: CD28-dependent superior eradication of solid tumors together with 41BB-dependent persistence of CAR T cells are achieved by co-administration of CD28 and 41BB CAR T cells rather than combining the two domains in a third generation CAR. (manuscript). [↗](#)
8. Volpin, V., Michels, T., Sorrentino, A., Menevse, A., Knoll, G., Ditz, M., Milenkovic, V., Chen, C., Rathinasamy, A., Griewank, K., Boutros, M., Haferkamp, S., Berneburg, M., Wetzel, C., Seckinger, A., Hose, D., Goldschmidt, H., Ehrenschrwender, M., Witzens-Harig, M., Szöör, Á., Vereb, G., Khandelwal, N., Beckhove, P.: CAMK1D Triggers Immune Resistance of Human Tumor Cells Refractory to Anti-PD-L1 Treatment. [Cancer Immunol. Res. 8 1163-1179, 2020.](#) (D1, IF: 11.151) [↗](#)

9. Vámosi, G., Friedländer, E., Ibrahim, S., Brock, R., Szöllősi, J., Vereb, G.: EGF Receptor Stalls upon Activation as Evidenced by Complementary Fluorescence Correlation Spectroscopy and Fluorescence Recovery after Photobleaching Measurements. [Int. J. Mol. Sci. 20 \(13\), 1-22, 2019.](#) (Q1, IF: 4.556) [↗](#)
10. Csaplár, M., Szöőr, Á., Vereb, G.: Dual costimulation with CD28 and 41BB yields chimeric antigen receptors that are highly mobile, spontaneously homo-oligomerize and exhibit enhanced synapse formation and activation compared to either CD28 or 41BB CARs. (manuscript). [↗](#)
11. Szöőr, Á., Rusznák P., Szöllősi J., Abken, H., Vereb, G.: Targeted antigens with higher mobility are collected to larger and more efficient synapses by CAR redirected T cells. (manuscript). [↗](#)